Journal of the Neurological Sciences 396 (2019) 94–101

Contents lists available at ScienceDirect

Journal of the Neurological Sciences

journal homepage: www.elsevier.com/locate/jns

Retinal microvasculature changes in amyloid-negative subcortical vascular cognitive impairment compared to amyloid-positive Alzheimer's disease

Na-Yeon Jung[a,b,c], Jong Chul Han[d], Yi Ting Ong[e], Carol Yim-lui Cheung[f], Christopher P. Chen[g], Tien Yin Wong[e], Hee Jin Kim[b,c], Yeo Jin Kim[b,c,h], Juyoun Lee[b,c,i], Jin San Lee[b,c,j], Young Kyoung Jang[b,c], Changwon Kee[d], Kyung Han Lee[k], Eun-Joo Kim[l], Sang Won Seo[b,c], Duk L. Na[b,c,*]

[a] Department of Neurology, Pusan National University Yangsan Hospital, Pusan National University School of Medicine and Research Institute for Convergence of Biomedical Science and Technology, Yangsan, Republic of Korea
[b] Department of Neurology, Samsung Medical Center, Sungkyunkwan University School of Medicine, Seoul, Republic of Korea
[c] Neuroscience Center, Samsung Medical Center, Seoul, Republic of Korea
[d] Department of Ophthalmology, Samsung Medical Center, Sungkyunkwan University School of Medicine, Seoul, Republic of Korea
[e] Singapore Eye Research Institute, Singapore National Eye Centre, Singapore
[f] Department of Ophthalmology & Visual Sciences, Chinese University of Hong Kong, Hong Kong
[g] Department of Pharmacology, National University of Singapore, Singapore
[h] Department of Neurology, Chuncheon Sacred Heart Hospital, Hallym University College of Medicine, Chuncheon, Republic of Korea
[i] Department of Neurology, Chungnam National University Hospital, Daejeon, Republic of Korea
[j] Department of Neurology, Kyung Hee University Hospital, Seoul, Republic of Korea
[k] Department of Nuclear Medicine, Samsung Medical Center, Sungkyunkwan University School of Medicine, Seoul, Republic of Korea
[l] Department of Neurology, Pusan National University Hospital, Pusan National University School of Medicine and Medical Research Institute, Busan, Republic of Korea

ARTICLE INFO

Keywords:
Retinal vessels
Alzheimer's disease
Vascular dementia
Amyloid
Cerebral small vessel diseases

ABSTRACT

Background and purpose: To investigate small vessel abnormalities in patients with cognitive impairment, we compared retinal microvascular alterations between patients with cognitive impairment related to Alzheimer's disease (ADCI) and those with subcortical vascular cognitive impairment (SVCI).

Methods: We prospectively recruited 29 amyloid-positive ADCI patients, 28 amyloid-negative SVCI patients that were confirmed by ^{11}C-PiB-PET scan and 34 individuals with normal cognition (NC). The three groups were compared in terms of retinal vascular variables (retinal fractal dimension, vascular caliber, tortuosity and branching angle) by using a semi-automated, computer-assisted analysis of digital fundus photographs. We also investigated the relationship between retinal variables and white matter hyperintensities (WMH) on MRI.

Results: Compared to NC individuals, the SVCI patients had smaller total and arteriolar fractal dimensions, whereas there was no significant difference of fractal dimension between ADCI and NC. Other retinal variables did not differ among the three groups. A significant correlation existed between fractal dimension and WMH volume.

Conclusions: Retinal microvascular alterations, especially retinal fractal dimension, may be useful markers that reflect cerebral microvascular changes in patients with SVCI as opposed to ADCI, who had no definite difference in retinal variables compared to the NC group.

1. Introduction

Alzheimer's disease (AD) and cerebrovascular disease (CVD) are the most common causes of dementia, accounting for as many as 70% of all dementia etiologies [1]. Therefore, the causes of dementia are often dichotomized into Alzheimer dementia and vascular dementia (VaD). However, these two disorders, especially AD and subcortical VaD (SVaD), largely overlap. CVD is present in 30–60% of AD brains in

Abbreviations: AD, Alzheimer's disease; SIVA, Singapore I vessel assessment; SVaD, subcortical vascular dementia

* Corresponding author at: Department of Neurology, Samsung Medical Center, Sungkyunkwan University School of Medicine, 81 Irwon-ro, Gangnam-gu, Seoul, 06351, Republic of Korea.
E-mail address: dukna@skku.edu (D.L. Na).

https://doi.org/10.1016/j.jns.2018.10.025
Received 25 April 2018; Received in revised form 25 October 2018; Accepted 29 October 2018
Available online 31 October 2018
0022-510X/

autopsy studies [2–5]. Conversely, as many as 88% of patients clinically diagnosed with VaD have an Alzheimer pathology (40% have pure AD, 40% have small vessel disease with AD and 8% have large vessel disease with AD) as assessed by autopsy [6].

Small vessel changes are considered a hallmark of what is referred to as subcortical vascular cognitive impairment (SVCI), a term that combines SVaD and its prodromal stage (subcortical vascular mild cognitive impairment). Cardiovascular risk factors contribute to obliterate small and medium sized cerebral arteries, resulting in lacunes, white matter hyperintensities (WMH) or microbleeds that are commonly observed on brain MRI in patients with SVCI [7]. However, microvascular abnormalities have also been reported to occur in patients with cognitive impairment related to Alzheimer's disease (ADCI), a combined condition of Alzheimer disease dementia and its prodromal stage, the amnestic type of mild cognitive impairment. That is, as Aβ accumulates in an Alzheimer brain, amyloid angiopathy involving small and medium sized arteries occurs [8], or elevated brain Aβ levels contribute to disrupt vascular components [9,10] leading to microvascular obstruction in ADCI patients.

Conventional MRI is useful in demonstrating small vessel disease markers such as lacunar infarction, WMH and microbleeds, as already discussed. DTI scans may show microstructural changes even before WMH become apparent. However, these changes would appear on MRI after small cerebral vessels have been obliterated or small vessels have had longstanding hypoperfusion. Thus, these changes only represent a relatively late stage of small vessel disease. Therefore, cerebral small vessels need to be visualized directly before overt change on MRI. As people age, they are more likely to have concomitant cerebrovascular pathology. The importance of detecting microvascular changes early cannot be stressed enough because CVD can be prevented with appropriate measures.

Recently retinal vessels were identified as a proxy of small brain vessels. Retinal vessels are anatomically similar and have the same developmental origin as small cerebral vessels [11,12]. Additionally, the morphology of retinal vascular structure can be identified in vivo with funduscopy. In patients with vascular cognitive impairment, such as subcortical vascular dementia and post-stroke dementia, several studies have shown an association between retinal vessel changes and lacunes or stroke [13,14]. However, as described already, AD pathology and small vessel disease often go hand in hand. About 30% of patients clinically diagnosed with SVaD have been reported to be positive for amyloid positron emission tomography (PET) [15], and this result has been replicated in other studies [16–18]. Because amyloid deposition may cause CVD through inflammatory pathways or by disrupting blood vessels [8], patients with mixed AD and CVD pathology must be excluded to identify the effects of CVD on retinal vasculature. More recent studies have also shown that retinal vessel variables are altered in patients clinically diagnosed with Alzheimer's disease [19,20]. However, as many as 12% of patients with clinically diagnosed AD can be amyloid negative in amyloid PET scans [18]; thus, the possibility of recruiting patients with non-AD dementia cannot be eliminated.

To exclude mixed dementia and non-AD pathology, we therefore recruited amyloid-positive ADCI patients, amyloid-negative SVCI patients and individuals with normal cognition (NC) and compared retinal microvascular alterations among the three groups.

2. Methods

2.1. Participants

ADCI in our sample consisted of amnestic mild cognitive impairment (aMCI) and probable AD dementia. SVCI consisted of subcortical vascular MCI (svMCI) and SVaD. Probable AD dementia patients fulfilled criteria proposed by the National Institute of Neurological and Communicative Disorders and Stroke and the AD and Related Disorders Association (NINCDS-ADRDA) [21]. Patients with SVaD met the diagnostic criteria for vascular dementia as determined by the Diagnostic and Statistical Manual of Mental Disorders–Fourth Edition (DSM-IV) and fulfilled imaging criteria for SVaD proposed by Erkinjuntti et al. [22]. aMCI and svMCI patients met Petersen's criteria for MCI with modifications as previously described [23]. All svMCI and SVaD patients had severe WMH on MRI scans, which was defined as a cap or band (periventricular WMH) ≥ 10 mm and deep white matter lesions (deep WMH) ≥ 25 mm, as modified from the Fazekas ischemia criteria [24].

Our initial sample consisted of 114 patients with clinically-defined ADCI and 137 patients with clinically-defined SVCI who had undergone detailed neuropsychological testing [25], MRI and [^{11}C] PiB-PET scan at Samsung Medical Center between September 2008 and May 2011. Of the 45 patients with aMCI and 69 patients with probable AD dementia, 28 (62.2%) and 61 (88.4%) patients, respectively (total ADCI = 89), tested amyloid positive by PiB-PET scan. Of the 67 patients with svMCI and 70 patients with SVaD, 47 (70.1%) and 45 (64.3%) patients, respectively (total SVCI = 92), were shown to be amyloid negative.

Of this initial sample, we contacted patients who visited our clinic between September 2014 and November 2015 when we performed fundus photography. Two PiB(−) svMCI patients were excluded from the study because of histories of optical conditions including branch retinal artery occlusion and macular degeneration. A total of 59 patients completed digital fundus photography, and consisted of 6 PiB(+) aMCI, 23 PiB(+) AD dementia, 19 PiB(−) svMCI, and 11 PiB(−) SVaD patients. Two PiB(−) svMCI patients were excluded from the final analysis because of poor retinal image quality (Fig. 1). Therefore, data from 57 patients was used in the final analysis.

Of the 89 amyloid-positive ADCI patients, those included (29/89) and excluded (60/89) did not differ in terms of age, sex, hypertension, diabetes mellitus, ischemic heart disease, stroke or hyperlipidemia. Only history of alcohol use and smoking were more frequent in excluded than included ADCI patients. Of the 92 amyloid-negative SVCI patients, those included (28/92) and excluded (64/92) did not differ in terms of age, sex, hypertension, diabetes mellitus, hyperlipidemia or smoking history. However, ischemic heart disease, stroke and history of alcohol use were more common in excluded than included SVCI patients (Supplementary Table 1).

For the control group, we recruited 34 individuals with subjective memory impairment (SMI) who underwent detailed neuropsychological testing and brain MRI at the Memory Clinic at Samsung Medical Center from January 2012 to June 2015. Inclusion criteria were: (i) subjective memory complaints by patients or caregivers; (ii) no objective cognitive dysfunction as evidenced by evaluation scores on any cognitive domains; and (iii) not suffering dementia. Exclusion criteria included history of traumatic brain injury, cortical stroke, seizure, brain surgery, current systemic medical disease that could affect cognition and severe WMH, defined as deep WMH ≥ 25 mm and periventricular WMH ≥ 10 mm. We also excluded individuals who met the Diagnostic and Statistical Manual of Mental Disorders (Fourth Edition) criteria for psychotic or mood disorders, such as schizophrenia or major depressive disorder [26].

We obtained written consent from each participant and the Institutional Review Board of Samsung Medical Center approved the study protocol (IRB No. 2014–07–030-008).

2.2. [^{11}C] PiB PET

All ADCI and SVCI patients completed a [^{11}C] PiB PET scan at Samsung Medical Center or Asan Medical Center using a Discovery STe PET/CT scanner (GE Medical Systems, Milwaukee, WI, USA) in 3-dimensional scanning mode that examined 35 slices of 4.25-mm thickness spanning the entire brain. [^{11}C] PiB was injected into the antecubital vein as a bolus injection with a mean dose of 420 MBq (i.e., range 259–550 MBq). Sixty minutes after injection, a CT scan was performed to correct for attenuation. A 30-minute emission static PET scan was

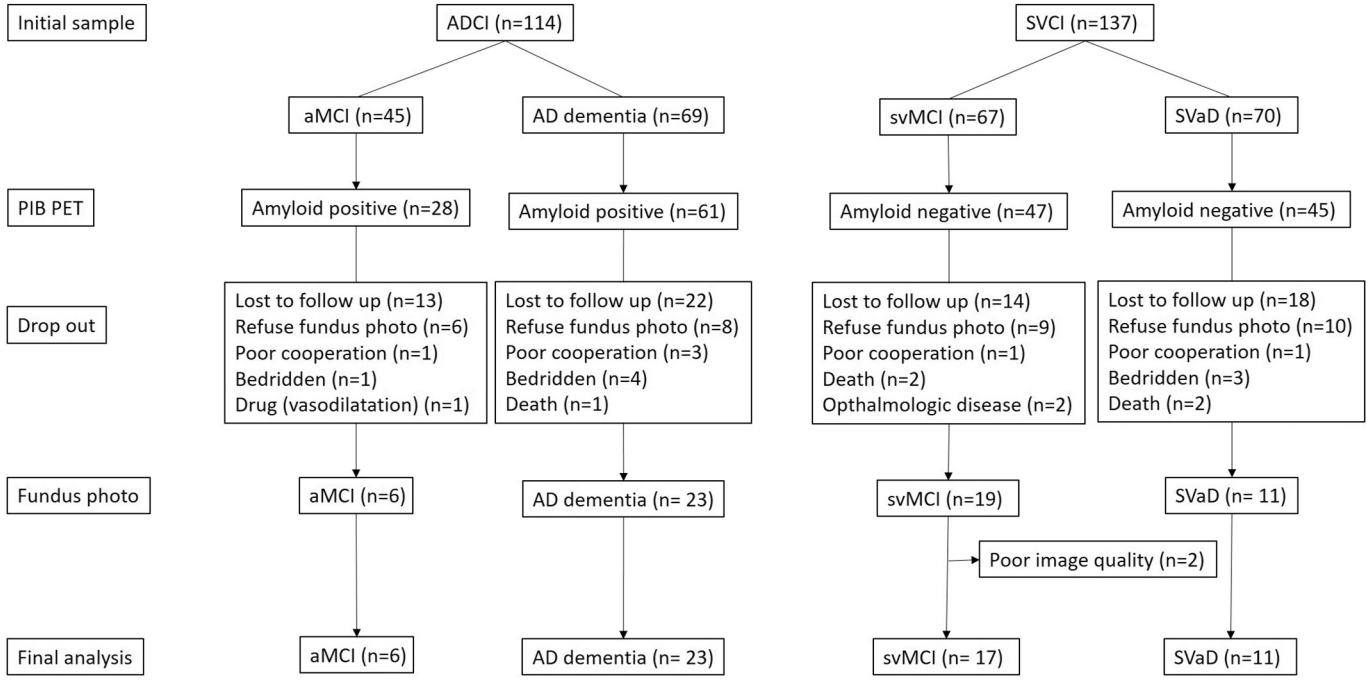

Fig. 1. Participant flow diagram.

then initiated. The specific radioactivity of [^{11}C] PiB at the time of administration was higher than 33.3 GBq/μmol. In all PET studies, the radiochemical purity of the radiotracer was higher than 95%.

PiB-PET images were co-registered to individual MRIs, which were normalized to a T1-weighted MRI template. Using these parameters, MRI co-registered PiB-PET images were normalized to the MRI template. Regional PiB retention values were quantified on spatially normalized PiB images by an automated VOI analysis using the automated anatomical labeling (AAL) atlas. Data were processed with SPM Version 5 (SPM5) in Matlab 6.5 (MathWorks, Natick, MA, USA).

To measure PiB retention, the cerebral cortical region was used to determine the cerebellum uptake ratio. The cerebellar gray matter was used as a reference region. Twenty-eight cortical VOIs from the left and right hemispheres were selected with the AAL atlas. The cerebral cortical VOIs chosen for this study consisted of the bilateral frontal, posterior cingulate gyri, parietal, lateral temporal and occipital regions. Regional cerebral cortical uptake ratios were calculated by dividing each cortical VOI uptake ratio by the mean uptake of the cerebellar cortex (cerebellum crus1 and crus2). Global PiB standardized uptake value ratio (SUVR) was calculated from the volume-weighted average uptake ratio of 28 bilateral cerebral cortical VOIs. Amyloid positive was defined if global SUVR was > 2 standard deviations (PiB SUVR above 1.5) from the mean of the normal controls [15,27].

2.3. Retinal photography and quantitative measurements of retinal microvasculature

Digital fundus photographs were collected with a 45° digital retinal camera (TRC-50DX; Topcon Medical Systems, Inc., USA) after pupil dilation with 1% tropicamide and 2.5% phenylephrine hydrochloride. A retinal image centered on the optic disc of each eye was obtained. Fundus images obtained at Samsung Medical Center Seoul Korea were sent to ocular research experts in Singapore who were blinded to the clinical information. The retinal image of the right eye was analyzed. If the right image was not suitable, the retinal image of the left eye was analyzed. Retinal vascular variables from photographs were quantified by a semi-automated, computer-assisted program (Singapore I Vessel Assessment [SIVA], software version 3.0). SIVA automatically recognizes the optic disc, arranges a grid with reference to the center of the optic disc, distinguishes vessel type, and calculates retinal vascular variables. Trained graders, masked to participant characteristics, visually evaluated the automated results and intervened manually if necessary according to a standardized protocol [28]. The graders determined the radius of the optic disk by marking 2 points corresponding to the center of the optic disk and the maximum vertical distance from the center of the optic disk to the margin of the optic disk edge. The measured area was defined within the region between 0.5 and 2.0 disc diameters away from the disc margin. The intra- and inter-grader reliability for the measurement have been reported previously [28].

2.3.1. Retinal vascular fractal dimension

Total, arteriolar, and venular fractal dimensions were computed from a skeletonized line tracing by using the box-counting method. With the box counting method, the retinal image was divided into a lot of equally sized square boxes, and the number of boxes containing a section of the line tracing was counted. The process was repeated with a different sized box. Fractal dimension is the slope of the line obtained via plotting the logarithm of the number of boxes through which the tracing passes against the logarithm of the size of the boxes. Fractal dimension was used to estimate the whole branching pattern of the retinal vascular tree [19]. Larger values indicate a more complex branching pattern.

2.3.2. Retinal vascular caliber

Retinal arteriolar and venular calibers were calculated and summarized as central retinal artery and central retinal vein equivalents, respectively [19]. The width of first branch of the largest six arterioles and venules were used in the calculation of average vessel width for computation of retinal vascular caliber. The retinal vascular caliber reflects the width of the red blood cell column.

2.3.3. Retinal vascular tortuosity

Retinal vascular tortuosity was measured as the integral of the curvature square along the vessel path normalized to the total path length; this represents a ratio measure [29]. The estimates were summarized as arteriolar and venular tortuosity, representing the average

tortuosity of arterioles and venules, respectively. Retinal vascular tortuosity shows the curliness of the vessels; a smaller tortuosity value indicates a straighter vessel [19].

2.3.4. Retinal vascular branching angle

Retinal vascular branching angle was determined as the first angle subtended between two daughter vessels at each vascular bifurcation [30]. Retinal arteriolar branching angle and retinal venular branching angle represent the average branching angle of arterioles and venules, respectively.

2.4. Blood pressure measurement

Blood pressure (BP) was measured concurrently before retinal photography on the same day with an automatic sphygmomanometer (Medical Electronics Sphygmomanometer TM-2655P; A&D Co. Ltd., Tokyo, Japan).

2.5. Neuropsychological tests

All patients underwent neuropsychological testing with a standardized battery called the Seoul Neuropsychological Screening Battery [25] at initial and follow-up assessment. However, neuropsychological data except for MMSE (Mini Mental State Examination) from only 50 (18 NC, 12 ADCI and 20 SVCI patients) of 91 patients was used in this study because the time gap between the neuropsychological tests and fundus photography was over one year in the other patients. The battery comprised tests for attention, language, calculation, praxis, visuospatial/constructive function, verbal/visual memory, and frontal/executive function as previously described [31]. Composite scores for attention, language and related functions, visuospatial, memory and frontal functions were calculated [32–34]. The attention score was calculated by summing the scores for the digit-span forward and digit-span backward tests (range: 0–17). The language and related function score was calculated by summing the scores from the Korean version of the Boston naming test (BNT) short form and calculation (range: 0–27). The visuospatial score was based on the Rey Complex Figure Test (RCFT) (range: 0–36). The memory score was calculated by summing scores from the verbal memory tests (SVLT immediate recall, delayed recall and recognition score) and visual memory tests (RCFT immediate recall, delayed recall and recognition score) (range: 0–144). The frontal score was calculated by summing scores from the category word generation (semantic Controlled Oral Word Association Test for animal), phonemic word generation and correct number in Stroop color-reading tests (range: 0–55).

2.6. Assessment of WMH volume

For WMH volume measurement, fist we obtained fluid attenuated inversion recovery (FLAIR) images as follows: axial slice thickness of 2 mm; no gap; repetition time of 11,000 ms; echo time of 125 ms; flip angle of 90°; and matrix size of 512 × 512 pixels. We then quantified WMH volume (in milliliters) on FLAIR images using Inbrain®, a Korea Food and Drug Administration (KFDA)-cleared software and a registered trademark of MIDAS Information Technology Co., Ltd. The automated WMH quantification process has been described in one of our previous studies [35]. All T1 weighted images were analyzed using FreeSurfer V6.0 with default parameters and the results were used in the process of creating a WMH region mask. FLAIR images were undergone nonuniformity correction, intensity normalization, and co-registration of FLAIR and T1 images of each subject. WMH was segmented using the FMRIB Automatic Segmentation Tool (FAST) algorithm with WMH candidate region mask on FLAIR images. By using intensity-substitution method, T1 images were classified into white matter and gray matter and localized into lobes properly. Periventricular WMH was defined in each slice via 10 mm dilation of the lateral ventricle mask and another region was defined as deep WMH region. Regionally localized atlases of the four lobes, and periventricular WMH and deep WMH were transformed into FLAIR native space and the WMH volume was quantified.

2.7. Statistical analyses

For descriptive statistics, we used the $\chi 2$ test or Fisher's exact test to compare dichotomous variables and analysis of variance followed by Bonferroni's post hoc analysis or Tukey's test using rank to compare continuous variables including retinal variables and WMH volume. Because total fractal dimension, arteriole fractal dimension, venular calibers, arteriolar tortuosity, and WMH volume were not normally distributed, we used Tukey's test using ranks to compare these variables. To control for covariates in the comparison of retinal variables, analysis of covariance (ANCOVA) was applied.

We used Spearman's correlation and multivariate linear regression to investigate correlation between retinal variables and WMH volume with adjustment for covariates that differed among the groups, including age, sex, hypertension, anti-platelet agent, body mass index (BMI) and APOE 4 carrier. We transformed total fractal dimension, arteriole fractal dimension, venular calibers, arteriolar tortuosity, and WMH volume using square root transformation for continuous analysis.

Multivariate linear regression models were performed for associations between retinal variables and group with adjustment for age, sex, hypertension, anti-platelet agent, body mass index (BMI) and APOE 4 carrier. Receiver operating characteristic (ROC) curves were used to determine the sensitivity, specificity, and area under the curve (AUC) of retinal variables for the discrimination of SVCI from ADCI, SVCI from NC, and ADCI from NC [36]. We used the Youden index [37] to identify an ideal cut-off for retina variables to discriminate each other. To find retinal variables that were significantly associated with cognitive function, Pearson correlations and multivariate linear regression analyses were performed after adjusting for age, sex and education for each retinal variable. Statistical analyses were conducted with SPSS version 21 (IBM Corp. Armonk, NY, USA). Statistical significance was defined as $p < .05$.

3. Results

3.1. Demographic and clinical characteristics

Demographic and clinical characteristics are shown in Table 1. Patients with SVCI were older and had higher prevalence of hypertension than did NC individuals. The three groups did not differ in systolic or diastolic BP at the time of fundus evaluation. The prevalence of diabetes among the three groups was not different, and diabetic retinopathy was not found in all individuals. The ADCI group had significantly more APOE 4 carriers than did the other groups. BMI was higher in the SVCI group than in the NC group. The three groups did not differ in sex, other vascular risk factors, alcohol history or smoking history. Patients with ADCI and SVCI had lower scores than did NC individuals on the MMSE and all cognitive domains of neuropsychological tests. The ADCI and SVCI groups did not differ in MMSE scores or any composite score of each cognitive domain, except for the memory domain. The SVCI group had larger WMH volume than the NC and ADCI groups, whereas WMH volume did not differ between the NC and ADCI groups.

3.2. Comparison of retinal variables between the normal cognition, ADCI and SVCI groups

Compared with the NC group, the SVCI group had smaller total and arteriolar fractal dimensions. Fractal dimensions did not differ significantly between the ADCI and NC groups. Other variables, such as retinal vascular caliber, tortuosity and branching angle did not differ among groups (Table 2, Fig. 2).

Table 1
Demographic and clinical characteristics of the study population.

	NC	ADCI	SVCI	*P* value NC vs. ADCI	P value NC vs. SVCI	P value ADCI vs SVCI
N	34	29	28			
Age, years	69.8 ± 6.1	73.8 ± 8.0	75.4 ± 8.0	0.109	0.011	1
Sex, female, n (%)	27 (79.4)	16 (55.2)	20 (71.4)	0.058	0.557	0.274
Vascular risk factors, n (%)						
Hypertension	13 (38.2)	11 (37.9)	25 (89.3)	1	< 0.001	< 0.001
Diabetes	2 (5.9)	1 (3.4)	5 (17.9)	1	0.228	0.102
Hyperlipidemia	17 (50.0)	9 (31.0)	10 (35.7)	0.199	0.309	0.783
Ischemic heart disease	4 (11.8)	1 (3.4)	0 (0)	0.363	0.120	1
Stroke	1 (2.9)	0 (0)	1 (3.6)	1	1	0.491
Alcohol (drinking)	9 (26.50)	7 (24.1)	9 (32.1)	1	0.780	0.565
Smoking (smoker)	6 (17.6)	4 (13.8)	6 (21.4)	0.741	0.755	0.504
Antiplatelet drug use, n (%)	14(41.2)	7 (24.1)	20 (71.4)	0.187	0.022	0.001
APOE E4 carrier, n (%) (n = 89)	11 (34.4)	23 (79.3)	6 (21.4)	0.001	0.390	< 0.001
Height, cm	156.6 ± 7.9	158.4 ± 10.3	153.0 ± 9.1	1	0.382	0.083
Weight, kg	57.2 ± 10.6	62.2 ± 11.1	58.9 ± 9.4	0.178	1	0.695
BMI, kg/m^2	23.2 ± 3.1	24.6 ± 2.3	25.1 ± 3.2	0.155	0.032	1
Systolic BP, mmHg	125.0 ± 16.2	128.0 ± 17.6	129.6 ± 15.8	1	0.815	1
Diastolic BP, mmHg	74.3 ± 9.6	75.0 ± 10.3	75.3 ± 11.0	1	1	1
MMSE	28.1 ± 2.0	18.0 ± 11.3	22.1 ± 5.6	< 0.001	0.005	0.108
Neuropsychological testing						
Attention(n = 50)	10.6 ± 2.8	7.9 ± 2.2	8.0 ± 1.7	0.007	0.002	1
Language(n = 43)	24.0 ± 1.9	18.6 ± 5.6	18.3 ± 6.0	0.015	0.003	1
Visuospatial(n = 49)	33.5 ± 1.5	26.0 ± 8.8	23.3 ± 10.1	0.043	0.001	1
Memory(n = 46)	83.8 ± 9.9	25.6 ± 15.3	55.0 ± 25.6	< 0.001	< 0.001	0.001
Frontal(n = 28)	42.5 ± 6.0	22.0 ± 15.5	22.5 ± 11.6	0.004	0.001	1
WMH volume (mm^3)						
Total	4710 (1730, 6820)	4684 (3362, 6715)	37,147 (29,155, 59,698)	0.378	< 0.001	< 0.001
Periventricular	3832 (1320, 6115)	3879 (3027, 6082)	30,297 (20,474, 47,585)	0.329	< 0.001	< 0.001
Deep	347 (218, 1015)	396 (172, 759)	5162 (3615, 8472)	0.933	< 0.001	< 0.001

We used the $\chi 2$ test or Fisher's exact test to compare dichotomous variables, and analysis of variance followed by Bonferroni's post hoc analysis to compare continuous variables except for WMH volume. Tukey's test using ranks was used for comparison of WMH volume. Continuous variables except for WMH volume are expressed as mean ± standard deviation. WMH volume is expressed as median (interquartile range).
Abbreviations: ADCI, cognitive impairment related to Alzheimer's disease; BMI, body mass index; BP, blood pressure; MMSE, Mini Mental State Examination; NC, normal cognition; SVCI, subcortical vascular cognitive impairment; WMH, white matter hyperintensities.

Multiple linear regression analyses were performed on the fractal dimension, showing that smaller fractal dimension correlated with SVCI even after controlling for age, sex, hypertension, antiplatelet drug, BMI and APOE genotype (Table 3). In the ADCI group, however, total fractal dimension was only mildly associated, and the association disappeared after controlling for APOE genotype.

Microvascular changes also occurred on the venous side. The SVCI group had a significantly decreased venular fractal dimension even after controlling for covariates including age, sex, hypertension, antiplatelet drug, APOE 4 and BMI (Supplementary Table 2), which was not the case for ADCI patients.

3.3. Correlation between retinal variables and WMH volume

For all participants, Spearman correlation coefficients between arteriolar fractal dimension and whole WMH volume was −0.345 (p = .001), while those between arteriolar fractal dimension and periventricular or deep WMH volume were −0.335 (p = .001) and −0.342 (p = .001), respectively. Total (arteriolar and venular combined) fractal dimension showed weak correlation with WMH. Spearman correlation coefficients for whole WMH volume, periventricular WMH volume, and deep WMH volume were −0.274 (p = .01), −0.264 (p = .013), and −0.278 (p = .009), respectively. In addition, Spearman correlation

Table 2
Comparison of retinal variables among the groups.

	NC	ADCI	SVCI	P value NC vs. ADCI	P value NC vs. SVCI	P value ADCI vs SVCI
Fractals						
Total fractal dimension	1.441 ± 0.047	1.411 ± 0.060	1.392 ± 0.062	0.143	0.002	0.242
Arteriolar fractal dimension	1.227 ± 0.050	1.199 ± 0.061	1.165 ± 0.070	0.214	< 0.001	0.057
Venular fractal dimension	1.214 ± 0.050	1.189 ± 0.056	1.181 ± 0.065	0.286	0.084	1
Caliber						
Central retinal artery equivalent, μm	149.64 ± 11.93	150.71 ± 10.97	151.52 ± 16.01	1	1	1
Central retinal vein equivalent, μm	212.68 ± 15.65	214.10 ± 13.68	218.91 ± 24.48	1	0.142	0.168
Tortuosity						
Arteriolar tortuosity ($\times 10^4$)	0.423 ± 0.073	0.428 ± 0.091	0.412 ± 0.013	0.999	0.915	0.908
Venular tortuosity ($\times 10^4$)	0.532 ± 0.096	0.533 ± 0.011	0.558 ± 0.011	1	1	1
Bifurcation						
Arteriolar branching angle, °	71.61 ± 11.61	75.69 ± 11.66	72.17 ± 11.03	0.485	1	0.745
Venular branching angle, °	76.71 ± 9.61	79.35 ± 8.08	74.74 ± 12.04	0.894	1	0.255

Analysis of variance (ANOVA) followed by Bonferroni's post hoc analysis or Tukey's was performed to compare retinal variables.
Abbreviations: ADCI, cognitive impairment related to Alzheimer's disease; NC, normal cognition; SVCI, subcortical vascular cognitive impairment.

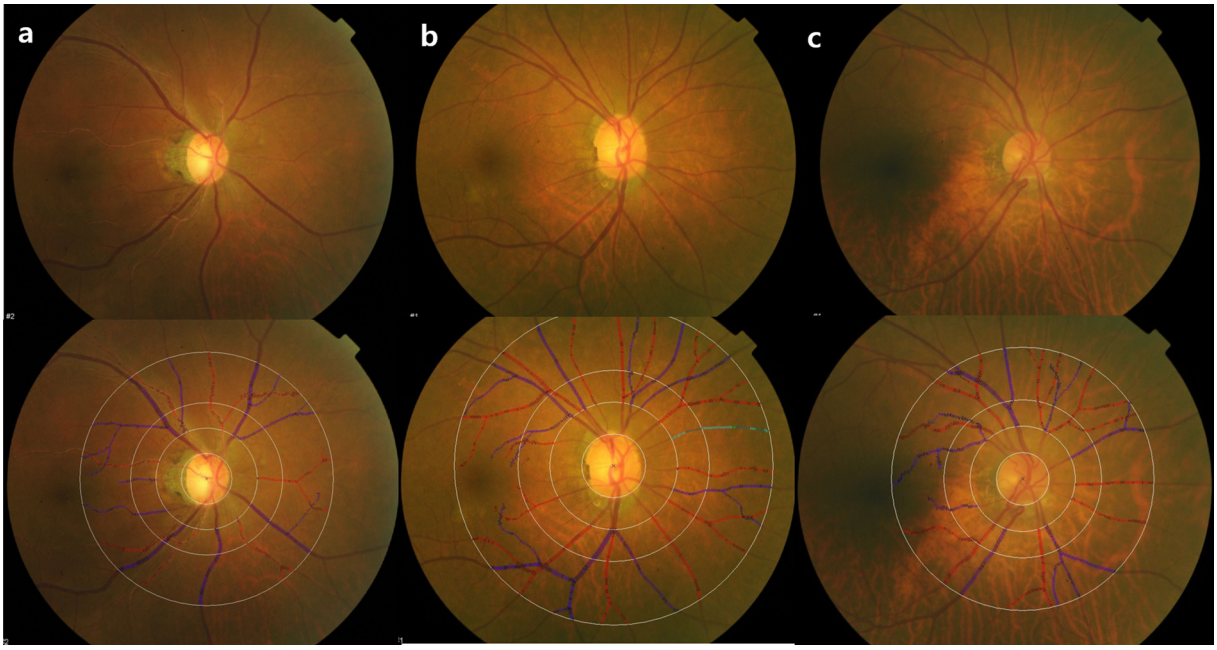

Fig. 2. Examples retinal images from a 61-year-old male amyloid negative SVaD (a), 74-year-old female normal cognition (b) and 75-year-old female amyloid positive AD (c). These examples show that fractal dimension of the SVaD patient (total fractal dimension, 1.391; arteriolar fractal dimension, 1.145) is smaller than that of the normal cognition individual (total fractal dimension, 1.499; arteriolar fractal dimension, 1.307) and the AD patient (total fractal dimension, 1.425; arteriolar fractal dimension, 1.240). Top images are original. Bottom images show the optic disc and vessel identified by the SIVA software. Arterioles are in red and venules in blue. (For interpretation of the references to color in this figure legend, the reader is referred to the web version of this article.)

Table 3
Multivariate analysis of the relationship between fractal dimension and ADCI and SVCI.

	ADCI (with NC as reference group)		SVCI (with NC as reference group)	
	β*	p value	β*	p value
Model 1				
Total fractal dimension (sqrt)	−6.030	0.024	−13.851	0.002
Arteriolar fractal dimension (sqrt)	−4.221	0.070	−10.537	0.004
Venular fractal dimension	−2.411	0.041	−4.998	0.009
Model 2				
Total fractal dimension (sqrt)	−2.959	0.258	−14.368	0.001
Arteriolar fractal dimension (sqrt)	−1.638	0.471	−10.524	0.005
Venular fractal dimension	−1.169	0.309	−5.605	0.005

Multiple linear regression analyses were applied ($p < .05$).
Model 1: age, sex, hypertension, anti-platelet agent and BMI were entered as independent factors.
Model 2: APOE 4 carrier was entered as an independent factor to Model 1.
Adjusted *P* values were derived by multiple regression. β denotes the regression coefficient in the multivariate model. *indicates unstandardized coefficient.
Abbreviations: ADCI, cognitive impairment related to Alzheimer's disease; NC, normal cognition; SVCI, subcortical vascular cognitive impairment; sqrt, square rood transformation.

coefficients between venular caliber and whole WMH volume and periventricular WMH volume were 0.228 ($p = .033$) and 0.229 ($p = .032$), respectively. However, there was no correlation between other retinal variables and WMH.

In multivariate linear regression, larger WMH volume was significantly correlated with smaller total fractal dimension and arteriole fractal dimension. Larger deep WHM volume was correlated with larger venular tortuosity (Supplementary Table 3).

3.4. Differential accuracy for each group

ROC curves were built to determine, for each retinal variable, the cut-off scores that best discriminated each group based on sensitivity and specificity values. For discriminating SVCI from NC, arteriole fractal dimension showed the best accuracy (AUC, 0.791; 95% confidence interval, CI, 0.669–0.884; sensitivity, 79%; specificity, 82%) at the cut-off 1.198. For discriminating SVCI from ADCI, arteriole fractal dimension showed the best accuracy (AUC, 0.654; 95% CI, 0.516–0.775; $p = .04$; sensitivity, 86%; specificity, 52%) at the cut-off 1.227. In terms of discriminating ADCI form NC, there was no significant model using ROC curves.

3.5. Correlation between retinal variables and cognitive function

Multivariate linear regression controlled for age, sex and education showed the combined group (NC, SVCI and ADCI) had a positive correlation between the total (arteriolar and venular combined) fractal dimension and language, total fractal dimension and visuospatial domains, arteriolar fractal dimension and language, and arteriolar fractal dimension and visuospatial domains (Table 4). However, when the same analysis was performed in each group separately, no retinal variables were associated with MMSE or any cognitive domain score. In

Table 4
Multivariate analysis of the relationship between fractal dimension and cognitive function in all participants.

	Attention (n = 50)		Language (n = 43)		Visuospatial (n = 49)		Memory (n = 46)		Frontal (n = 28)		MMSE (*n* = 91)	
	β	p value	β	p value	β	p value	β	p value	β	p value	β	p value
Total fractal dimension (sqrt)	1.4	0.928	56.8	0.035	131.6	0.015	−206.7	0.377	105.7	0.528	38.2	0.194
Arteriolar fractal dimension (sqrt)	−2.4	0.835	44.8	0.026	123.6	0.002	−96.5	0.593	133.2	0.262	47.4	0.051
Venular fractal dimension	−3.6	0.587	19.0	0.116	24.8	0.311	−160.1	0.096	−58.9	0.405	6.9	0.589

Multiple linear regression analyses were performed adjusting for age, sex and education. Adjusted P values were derived by multiple regression. β denotes the regression coefficient in the multivariate model.
Abbreviations: MMSE, Mini Mental State Examination; sqrt, square rood transformation.

the SVCI group, the Pearson correlation coefficient between arteriolar fractal dimension and visuospatial composite score was 0.475 at the 0.05 level.

4. Discussion

Herein, we compared retinal variables among NC, PiB(+) ADCI and PiB(−) SVCI groups. We found that: (1) the fractal dimension of retinal vasculature was smaller in the SVCI group compared to the NC group; (2) arteriolar fractal dimension was inversely correlated with WMH volumes in the whole group; (3) retinal variables including fractal dimension did not differ significantly between the ADCI and either NC or SVCI group; and (4) fractal dimensions were associated with language and visuospatial functions in the entire study population.

The smaller fractal dimension in the SVCI group compared to the NC group suggests that arteriolar fractal dimension can be a biomarker of small vessel disease (SVD) in patients with vascular cognitive impairment. The accuracy of discriminating SVCI from NC in terms of arteriolar fractal dimension was fair (AUC 0.791) in our participants. Previous studies involving lacunar stroke or SVD showed similar findings [14,38,39], but to our knowledge, our study is the first to provide evidence that the fractal dimension in retinal arterioles and venules is decreased in patients with svMCI and SVaD. Fractal analysis is a measure of the branching complexity of structures and complex geometric patterns [39]. Retinal vascular fractal dimension is a reflection of its optimality and efficiency of blood distribution [40]. A reduction from optimal architecture can result in impaired microcirculatory transport and reduced blood flow efficiency with increased energy cost, which may increase the risk of CVD [12].

In all participants, WMH volume was inversely correlated with arteriole fractal dimension. WMH lesion is known to be caused by microvascular change due to arteriosclerosis or chronic ischemia due to hypoperfusion and disturbances of cerebral blood flow [8]. Our results suggested that retinal arteriole fractal dimension can reflect the state of cerebral small vessels. This finding is partially in line with the previous studies, which revealed that retinal arteriolar abnormalities correlated with MRI signs of cerebral white matter lesions in healthy people and patients with stroke or myocardial infarction [41–43]. However, those studies investigated on retinal narrowing, arteriolar geometry, microaneurysm, retinal hemorrhage, and presence of retinal exudates. There were few studies that showed the correlation of retinal fractal dimension and WMH volume in patients with cognitive impairment.

On the other hand, retinal variables did not differ between the ADCI and NC groups, although the ADCI and SVCI groups were at a comparable disease stage as assessed by detailed neuropsychological tests. In fact, the ADCI group had worse memory performance than did the SVCI group. The accuracy of discriminating ADCI from NC was not effective, either. These findings were not compatible with previous studies showing that there were smaller fractal dimensions, reduced branching complexity and narrowed veins in AD patients [19,44]. These discrepancies remain to be resolved. However, differences in inclusion criteria among studies can contribute, at least in part. Firstly, we used detailed neuropsychological tests to diagnose patients, whereas the previous study enrolled the cognitive dysfunction group by using a brief screening tool. Secondly, we selected ADCI patients with minimal ischemia on MRI and, more importantly, amyloid deposits on a PIB-PET scan, therefore excluding patients with non-AD pathology and vascular cognitive impairment. Thirdly, our sample size was also relatively small compared with previous studies. Another discrepancy between previous studies and our study was that the previous studies showed a positive association between cognition and fractal dimension [19,45] whereas our study found no association between neuropsychological tests and fractal dimension. Again, this discrepancy can be explained by the different inclusion criteria and sample size.

We found microvascular abnormalities extended to the venous side in our SVCI patients, showing that venular fractal dimension decreased, even after controlling for covariates. The majority of previous studies on vascular cognitive impairment have focused on arteriosclerotic change and arteriopathies [8], whereas only a few studies have given attention to venous or venular changes. Autopsy studies have shown that leukoaraiosis or confluent white matter lesions are associated with periventricular venous collagenosis, which is excessive collagen deposition in the walls of veins and venules [46]. Periventricular venous collagenosis used to be mistaken for hyalinized arterioles when routine stains were used; however, specific stains showed the affected vessels to be venules rather than arterioles [47]. Severe venous wall thickening in leukoaraiosis lesions results in narrow lumina and occlusion, causing venous insufficiency [48]. An animal study also revealed that arterial hypertension affects the venous system of brain and venous collagenosis [49].

Our study has limitations. First, as stated already, our sample size was relatively small compared with previous studies. Second, our NC group was composed of SMI individuals without PiB PET data. Therefore, we cannot completely exclude the possibility that there had been some preclinical AD in the NC group. Third, out of initial ADCI group we recruited only 33% of the patients. Despite these limitations, however, this study is the first to investigate retinal microvasculature in individuals with SVCI and ADCI who had undergone amyloid PET imaging, and the first study to reveal that patients with amyloid-negative SVCI had smaller fractal dimension on fundus photography. Retinal fractal dimension can be a noninvasive, inexpensive and useful way to detect SVCI. Our findings support the need for research on potential tests to identify people with SVCI who can try to modify risk factors at an early stage. The amyloid-positive ADCI group had no difference in retinal variables compared to the NC group. Because in vivo human studies to directly observe cerebral microvasculature are extremely rare, our results provide more precise insights into the pathomechanism of AD at the level of the neurovascular unit.

Acknowledgements

This study was supported by a grant of the Korean Health Technology R&D Project, Ministry of Health & Welfare, Republic of Korea (HI14C2746).

Conflicts of interest

The authors declare that they have no conflict of interest.

Appendix A. Supplementary data

Supplementary data to this article can be found online at https://doi.org/10.1016/j.jns.2018.10.025.

References

[1] W.M. van der Flier, P. Scheltens, Epidemiology and risk factors of dementia, J. Neurol. Neurosurg. Psychiatry 76 (Suppl. 5) (2005) v2–v7.
[2] K.A. Jellinger, Understanding the pathology of vascular cognitive impairment, J. Neurol. Sci. 229–230 (2005) 57–63.
[3] J.A. Schneider, Z. Arvanitakis, W. Bang, D.A. Bennett, Mixed brain pathologies account for most dementia cases in community-dwelling older persons, Neurology 69 (24) (2007) 2197–2204.
[4] J.A. Schneider, P.A. Boyle, Z. Arvanitakis, J.L. Bienias, D.A. Bennett, Subcortical infarcts, Alzheimer's disease pathology, and memory function in older persons, Ann. Neurol. 62 (1) (2007) 59–66.
[5] L.S. Honig, W. Kukull, R. Mayeux, Atherosclerosis and AD: analysis of data from the US National Alzheimer's Coordinating Center, Neurology 64 (3) (2005) 494–500.
[6] R.N. Kalaria, Neuropathological diagnosis of vascular cognitive impairment and vascular dementia with implications for Alzheimer's disease, Acta Neuropathol. 131 (5) (2016) 659–685.
[7] J. Staals, T. Booth, Z. Morris, M.E. Bastin, A.J. Gow, J. Corley, P. Redmond, J.M. Starr, I.J. Deary, J.M. Wardlaw, Total MRI load of cerebral small vessel disease and cognitive ability in older people, Neurobiol. Aging 36 (10) (2015) 2806–2811.
[8] K.A. Jellinger, Pathology and pathogenesis of vascular cognitive impairment-a critical update, Front. Aging Neurosci. 5 (2013) 17.
[9] A. Gupta, C. Iadecola, Impaired Abeta clearance: a potential link between atherosclerosis and Alzheimer's disease, Front. Aging Neurosci. 7 (2015) 115.
[10] M. Sole, A.J. Minano-Molina, M. Unzeta, Cross-talk between Abeta and endothelial SSAO/VAP-1 accelerates vascular damage and Abeta aggregation related to CAA-AD, Neurobiol. Aging 36 (2) (2015) 762–775.
[11] T.Y. Wong, R. Klein, B.E. Klein, J.M. Tielsch, L. Hubbard, F.J. Nieto, Retinal microvascular abnormalities and their relationship with hypertension, cardiovascular disease, and mortality, Surv. Ophthalmol. 46 (1) (2001) 59–80.
[12] N. Patton, T. Aslam, T. Macgillivray, A. Pattie, I.J. Deary, B. Dhillon, Retinal vascular image analysis as a potential screening tool for cerebrovascular disease: a rationale based on homology between cerebral and retinal microvasculatures, J. Anat. 206 (4) (2005) 319–348.
[13] S. Hilal, Y.T. Ong, C.Y. Cheung, C.S. Tan, N. Venketasubramanian, W.J. Niessen, H. Vrooman, A.R. Anuar, M. Chew, C. Chen, T.Y. Wong, M.K. Ikram, Microvascular network alterations in retina of subjects with cerebral small vessel disease, Neurosci. Lett. 577 (2014) 95–100.
[14] M. Cavallari, T. Falco, M. Frontali, S. Romano, F. Bagnato, F. Orzi, Fractal analysis reveals reduced complexity of retinal vessels in CADASIL, PLoS One 6 (4) (2011) e19150.
[15] J.H. Lee, S.H. Kim, G.H. Kim, S.W. Seo, H.K. Park, S.J. Oh, J.S. Kim, H.K. Cheong, D.L. Na, Identification of pure subcortical vascular dementia using 11C-Pittsburgh compound B, Neurology 77 (1) (2011) 18–25.
[16] B.S. Ye, S.W. Seo, J.H. Kim, G.H. Kim, H. Cho, Y. Noh, H.J. Kim, C.W. Yoon, S.Y. Woo, S.H. Kim, H.K. Park, S.T. Kim, Y.S. Choe, K.H. Lee, J.S. Kim, S.J. Oh, C. Kim, M. Weiner, J.H. Lee, D.L. Na, Effects of amyloid and vascular markers on cognitive decline in subcortical vascular dementia, Neurology 85 (19) (2015) 1687–1693.
[17] G.H. Kim, J.H. Lee, S.W. Seo, B.S. Ye, H. Cho, H.J. Kim, Y. Noh, C.W. Yoon, J.H. Chin, J. Oh, J.S. Kim, Y.S. Choe, K.H. Lee, S.T. Kim, J.H. Jeong, D.L. Na, Seoul criteria for PiB(−) subcortical vascular dementia based on clinical and MRI variables, Neurology 82 (17) (2014) 1529–1535.
[18] R. Ossenkoppele, W.J. Jansen, G.D. Rabinovici, D.L. Knol, W.M. van der Flier, B.N. van Berckel, P. Scheltens, P.J. Visser, P.E.T.S.G. Amyloid, S.C. Verfaillie, M.D. Zwan, S.M. Adriaanse, A.A. Lammertsma, F. Barkhof, W.J. Jagust, B.L. Miller, H.J. Rosen, S.M. Landau, V.L. Villemagne, C.C. Rowe, D.Y. Lee, D.L. Na, S.W. Seo, M. Sarazin, C.M. Roe, O. Sabri, H. Barthel, N. Koglin, J. Hodges, C.E. Leyton, R. Vandenberghe, K. van Laere, A. Drzezga, S. Forster, T. Grimmer, P. Sanchez-Juan, J.M. Carril, V. Mok, V. Camus, W.E. Klunk, A.D. Cohen, P.T. Meyer, S. Hellwig, A. Newberg, K.S. Frederiksen, A.S. Fleisher, M.A. Mintun, D.A. Wolk, A. Nordberg, J.O. Rinne, G. Chetelat, A. Lleo, R. Blesa, J. Fortea, K. Madsen, K.M. Rodrigue, D.J. Brooks, Prevalence of amyloid PET positivity in dementia syndromes: a meta-analysis, JAMA 313 (19) (2015) 1939–1949.
[19] C.Y. Cheung, Y.T. Ong, M.K. Ikram, S.Y. Ong, X. Li, S. Hilal, J.A. Catindig, N. Venketasubramanian, P. Yap, D. Seow, C.P. Chen, T.Y. Wong, Microvascular network alterations in the retina of patients with Alzheimer's disease, Alzheimer's & Dementia: J. Alzheimer's Assoc. 10 (2) (2014) 135–142.
[20] S. Frost, Y. Kanagasingam, H. Sohrabi, J. Vignarajan, P. Bourgeat, O. Salvado, V. Villemagne, C.C. Rowe, S.L. Macaulay, C. Szoeke, K.A. Ellis, D. Ames, C.L. Masters, S. Rainey-Smith, R.N. Martins, A.R. Group, Retinal vascular biomarkers for early detection and monitoring of Alzheimer's disease, Transl. Psychiatry 3 (2013) e233.
[21] G. McKhann, D. Drachman, M. Folstein, R. Katzman, D. Price, E.M. Stadlan, Clinical diagnosis of Alzheimer's disease: report of the NINCDS-ADRDA Work Group under the auspices of Department of Health and Human Services Task Force on Alzheimer's Disease, Neurology 34 (7) (1984) 939–944.
[22] T. Erkinjuntti, D. Inzitari, L. Pantoni, A. Wallin, P. Scheltens, K. Rockwood, G.C. Roman, H. Chui, D.W. Desmond, Research criteria for subcortical vascular dementia in clinical trials, J. Neural Transm. Suppl. 59 (2000) 23–30.
[23] S.W. Seo, S.S. Cho, A. Park, J. Chin, D.L. Na, Subcortical vascular versus amnestic mild cognitive impairment: comparison of cerebral glucose metabolism, J. Neuroimag.: Offl. J. Am. Soc. Neuroimag. 19 (3) (2009) 213–219.
[24] F. Fazekas, R. Kleinert, H. Offenbacher, R. Schmidt, G. Kleinert, F. Payer, H. Radner, H. Lechner, Pathologic correlates of incidental MRI white matter signal hyperintensities, Neurology 43 (9) (1993) 1683–1689.
[25] Y. Kang, D.L. Na, Seoul Neuropsychological Screening Battery, Human Brain Research & Consulting Co., Incheon, 2003.
[26] American Psychiatric Association, Diagnostic and statistical manual of mental disorders : DSM-IV, American Psychiatric Association, Washington, DC, 1994.
[27] H. Cho, S.W. Seo, J.H. Kim, M.K. Suh, J.H. Lee, Y.S. Choe, K.H. Lee, J.S. Kim, G.H. Kim, Y. Noh, B.S. Ye, H.J. Kim, C.W. Yoon, J. Chin, D.L. Na, Amyloid deposition in early onset versus late onset Alzheimer's disease, J. Alzheimer's Dis.: JAD 35 (4) (2013) 813–821.
[28] C.Y. Cheung, W.T. Tay, P. Mitchell, J.J. Wang, W. Hsu, M.L. Lee, Q.P. Lau, A.L. Zhu, R. Klein, S.M. Saw, T.Y. Wong, Quantitative and qualitative retinal microvascular characteristics and blood pressure, J. Hypertens. 29 (7) (2011) 1380–1391.
[29] W.E. Hart, M. Goldbaum, B. Cote, P. Kube, M.R. Nelson, Measurement and classification of retinal vascular tortuosity, Int. J. Med. Inform. 53 (2–3) (1999) 239–252.
[30] M. Zamir, J.A. Medeiros, T.K. Cunningham, Arterial bifurcations in the human retina, J. Gen. Physiol. 74 (4) (1979) 537–548.
[31] S.W. Seo, K. Im, J.M. Lee, Y.H. Kim, S.T. Kim, S.Y. Kim, D.W. Yang, S.I. Kim, Y.S. Cho, D.L. Na, Cortical thickness in single- versus multiple-domain amnestic mild cognitive impairment, NeuroImage 36 (2) (2007) 289–297.
[32] H.J. Ahn, J. Chin, A. Park, B.H. Lee, M.K. Suh, S.W. Seo, D.L. Na, Seoul Neuropsychological Screening Battery-Dementia version (SNSB-D): a useful tool for assessing and monitoring cognitive impairments in dementia patients, J. Korean Med. Sci. 25 (7) (2010) 1071–1076.
[33] H.J. Kim, K. Im, H. Kwon, J.M. Lee, C. Kim, Y.J. Kim, N.Y. Jung, H. Cho, B.S. Ye, Y. Noh, G.H. Kim, E.D. Ko, J.S. Kim, Y.S. Choe, K.H. Lee, S.T. Kim, J.H. Lee, M. Ewers, M.W. Weiner, D.L. Na, S.W. Seo, Clinical effect of white matter network disruption related to amyloid and small vessel disease, Neurology 85 (1) (2015) 63–70.
[34] B.S. Ye, S.W. Seo, G.H. Kim, Y. Noh, H. Cho, C.W. Yoon, H.J. Kim, J. Chin, S. Jeon, J.M. Lee, J.K. Seong, J.S. Kim, J.H. Lee, Y.S. Choe, K.H. Lee, Y.H. Sohn, M. Ewers, M. Weiner, D.L. Na, Amyloid burden, cerebrovascular disease, brain atrophy, and cognition in cognitively impaired patients, Alzheimer's & Dement.: J. Alzheimer's Assoc. 11 (5) (2015) 494–503 (e3).
[35] S. Jeon, U. Yoon, J.-S. Park, S.W. Seo, J.-H. Kim, S.T. Kim, S.I. Kim, D.L. Na, J.-M. Lee, Fully automated pipeline for quantification and localization of white matter hyperintensity in brain magnetic resonance image, Int. J. Imaging Syst. Technol. 21 (2) (2011) 193–200.
[36] D. Mossman, E. Somoza, ROC curves, test accuracy, and the description of diagnostic tests, J. Neuropsych. Clin. Neurosci. 3 (3) (1991) 330–333.
[37] W.J. Youden, Index for rating diagnostic tests, Cancer 3 (1) (1950) 32–35.
[38] N. Cheung, G. Liew, R.I. Lindley, E.Y. Liu, J.J. Wang, P. Hand, M. Baker, P. Mitchell, T.Y. Wong, R. Multi-Center, G. Stroke Study, Collaborative, retinal fractals and acute lacunar stroke, Ann. Neurol. 68 (1) (2010) 107–111.
[39] F.N. Doubal, T.J. MacGillivray, N. Patton, B. Dhillon, M.S. Dennis, J.M. Wardlaw, Fractal analysis of retinal vessels suggests that a distinct vasculopathy causes lacunar stroke, Neurology 74 (14) (2010) 1102–1107.
[40] T.F. Sherman, On connecting large vessels to small. The meaning of Murray's law, J. Gen. Physiol. 78 (4) (1981) 431–453.
[41] F.N. Doubal, R. de Haan, T.J. MacGillivray, P.E. Cohn-Hokke, B. Dhillon, M.S. Dennis, J.M. Wardlaw, Retinal arteriolar geometry is associated with cerebral white matter hyperintensities on magnetic resonance imaging, Int. J. Stroke: Offl. J. Int. Stroke Soc. 5 (6) (2010) 434–439.
[42] V.I. Kwa, J.J. van der Sande, J. Stam, N. Tijmes, J.L. Vrooland, G. Amsterdam Vascular Medicine, Retinal arterial changes correlate with cerebral small-vessel disease, Neurology 59 (10) (2002) 1536–1540.
[43] T.Y. Wong, R. Klein, A.R. Sharrett, D.J. Couper, B.E. Klein, D.P. Liao, L.D. Hubbard, T.H. Mosley, A.I.A.R.I.C. Study, Cerebral white matter lesions, retinopathy, and incident clinical stroke, JAMA 288 (1) (2002) 67–74.
[44] F. Berisha, G.T. Feke, C.L. Trempe, J.W. McMeel, C.L. Schepens, Retinal abnormalities in early Alzheimer's disease, Invest. Ophthalmol. Vis. Sci. 48 (5) (2007) 2285–2289.
[45] Y.T. Ong, S. Hilal, C.Y. Cheung, X. Xu, C. Chen, N. Venketasubramanian, T.Y. Wong, M.K. Ikram, Retinal vascular fractals and cognitive impairment, Dement. Geriatr. Cogn. Disord. Extra 4 (2) (2014) 305–313.
[46] D.M. Moody, W.R. Brown, V.R. Challa, R.L. Anderson, Periventricular venous collagenosis: association with leukoaraiosis, Radiology 194 (2) (1995) 469–476.
[47] W.R. Brown, C.R. Thore, Review: cerebral microvascular pathology in ageing and neurodegeneration, Neuropathol. Appl. Neurobiol. 37 (1) (2011) 56–74.
[48] S. Black, F. Gao, J. Bilbao, Understanding white matter disease: imaging-pathological correlations in vascular cognitive impairment, Stroke 40 (3 Suppl) (2009) S48–S52.
[49] M. Zhou, L. Mao, Y. Wang, Q. Wang, Z. Yang, S. Li, L. Li, Morphologic changes of cerebral veins in hypertensive rats: venous collagenosis is associated with hypertension, J. Stroke Cerebrovasc. Dis.: Offl. J Natl. Stroke Assoc. 24 (3) (2015) 530–536.